Chem Biol Drug Des 2013; **81:** 474–483

Research Article

Discovery of Thiazolidine-2,4-Dione/Biphenylcarbonitrile Hybrid as Dual PPAR α/γ Modulator with Antidiabetic Effect: *In vitro, In Silico* and *In Vivo* Approaches†

Sergio Hidalgo-Figueroa[1], Juan J. Ramírez-Espinosa[1], Samuel Estrada-Soto[1], Julio C. Almanza-Pérez[2], Rubén Román-Ramos[2], Francisco J. Alarcón-Aguilar[2], Jesús V. Hernández-Rosado[3], Hermenegilda Moreno-Díaz[4], Daniel Díaz-Coutiño[4] and Gabriel Navarrete-Vázquez[1,*]

[1]Facultad de Farmacia, Universidad Autónoma del Estado de Morelos, Av. Universidad 1001, Chamilpa, Cuernavaca Mor., 62209, México
[2]Laboratorio de Farmacología, Depto. Ciencias de la Salud, D.C.B.S., Universidad Autónoma Metropolitana-Iztapalapa, Apdo.-Postal 55–535, CP 09340, México, D.F., México
[3]Posgrado en Biología Experimental, D.C.B.S., Universidad Autónoma Metropolitana-Iztapalapa, Apdo.-Postal 55–535, CP 09340, México, D.F., México
[4]Universidad del Papaloapan, Campus Tuxtepec, Circuito Central 200, Col. Parque Industrial, 68301, Tuxtepec, Oaxaca, México
**Corresponding author: Gabriel Navarrete-Vázquez, gabriel_navarrete@uaem.mx*
†This work was taken in part from the PhD thesis of S. Hidalgo-Figueroa. He is a CONACyT fellow (209159). Vladimir Hernandez-Rosado is also a CONACYT fellow. We are grateful to Korina Sánchez-Salazar for technical assistance.

A small series of thiazolidine-2,4-dione and barbituric acid derivatives 1–4 was prepared using a short synthetic route, and all compounds were characterized by elemental analysis, mass spectrometry, and NMR (^{1}H, ^{13}C) spectroscopy. Their in vitro relative expression of peroxisome proliferator-activated receptor α and peroxisome proliferator-activated receptor γ was evaluated. Compound 1 showed an increase in the mRNA expression of both peroxisome proliferator-activated receptor isoforms, as well as the GLUT-4 levels. The antidiabetic activity of compound 1 was determined at 50 mg/kg single dose using a non-insulin-dependent diabetes mellitus rat model. The results indicated a significant decrease in plasma glucose levels. Additionally, we performed a molecular docking of compound 1 into the ligand binding pocket of peroxisome proliferator-activated receptor α and peroxisome proliferator-activated receptor γ. In these binding models, compound 1 may bind into the active site of both isoforms showing important short contacts with the peroxisome proliferator-activated receptor γ residues: Tyr 473, His 449, Ser 289, His 323; and peroxisome proliferator-activated receptor α residues: Tyr 464, His 440, Ser 280 and Tyr 314.

Key words: 2,4-thiazolidinedione, diabetes, dual agonist, hydrogen bonds, molecular docking, PPAR

Received 8 November 2012, revised 6 December 2012 and accepted for publication 10 December 2012

Peroxisome proliferator-activated receptors (PPARs) are ligand-activated transcription factors and members of the nuclear hormone receptor superfamily, and exist in three isoforms, PPARα, PPARγ, and PPARδ. Each of these regulates tissue-specific target genes involved in many biological processes such as the solute carrier family 2 (facilitated glucose transporter), member 4 (GLUT4) (1). PPARα and PPARγ are the molecular targets of a number of marketed drugs, such as the fibrate class of hypolipidemic drugs and the thiazolidinedione class of insulin-sensitizing drugs, respectively (2,3).

Cardiovascular disorders are the most common cause of morbidity and mortality in diabetes as well as dyslipidemic conditions, and their prevalence is increasing constantly in developing countries (4). Diabetes mellitus is a chronic and progressive disease of metabolic deregulation characterized by insulin resistance in peripheral tissues (liver, muscle, and adipose) and impaired insulin secretion by the pancreas (5).

Synchronized therapies, which concurrently control diabetes and inhibit progression of cardiovascular complications, may be a fascinating therapeutic option in the treatment of diabetes. PPAR α/γ dual agonists are new class of drugs, which have been developed to target both PPARs simultaneously to produce both antidiabetic and hypolipidemic effects (6). The recently investigated PPAR α/γ dual agonist tesaglitazar (Figure 1) is noted to reduce triglycerides, raise cardioprotective HDL levels and consequently improve insulin sensitivity (7,8).

© 2013 John Wiley & Sons A/S. doi: 10.1111/cbdd.12102

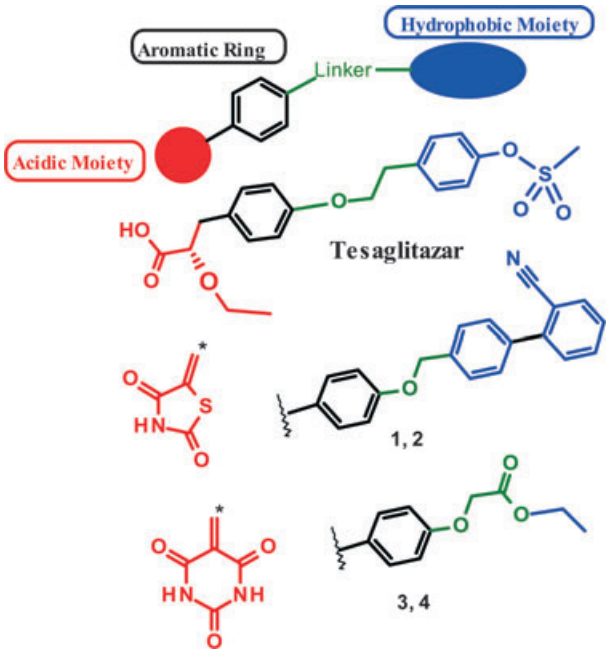

Figure 1: Pharmacophoric pattern in peroxisome proliferator-activated receptor (PPAR) α/γ dual agonist tesaglitazar and the requirements completed by compounds **1**–**4**.

The classic pharmacophoric features of PPAR α/γ dual agonists essentially consists of three parts (9): (i) an acidic head group, (ii) central aromatic region and, (iii) a lipophilic side chain (Figure 1).

The 2,4-thiazolidinedione ring in the most of glitazones is reported to make three central H-bonds with His323, Tyr473, and His449 that are important for the activation of the PPARγ. Several replacements of this heterocycle have been carried out using a variety of isosteres such as free carboxyl group, oxazolidinedione, tetrazole, and barbituric acid (9–11).

In our ongoing research on PPAR α/γ dual agonists derivatives with cardioprotective and antidiabetic activities, we report in this article the preparation of derivatives **1**–**4**, their *in vitro* relative expression of PPARα, PPARγ, and GLUT4, molecular docking of the most active compound in both PPAR isoforms, as well as its *in vivo* hypoglycemic effect.

Methods and Materials

Chemistry

All starting materials and reagents were obtained commercially and were used as received. Melting points were determined on an EZ-Melt MPA120 automated melting point apparatus from Stanford Research Systems and are uncorrected. TLC monitored reactions on 0.2 mm precoated silica gel 60 F254 plates (E. Merck KGaA, Darmstadt, Germany). NMR studies were carried out with a Varian Inova 400 instrument. Chemical shifts (δ_H, δ_C) and coupling constants values (J) are given in ppm and Hz, respectively. Standard reference was used: TMS ($\delta_H = 0$, $\delta_C = 0$) in DMSO-d_6. The following abbreviations are used: s, singlet; d, doublet; q, quartet; t, triplet; bs, broad signal. IR spectra have been recorded on a Bruker Vector 22 FT spectrophotometer (Bruker Instruments, Billerica, MA, USA). Mass spectra were recorded on a Jeol JMS-700 equipment (JEOL USA Inc., Peabody, MA, USA). Elemental analyses were carried out on an Elementar Vario ELIII instrument (Elementar, Hanau, Germany).

General method of synthesis of compounds 1–4

A mixture of 4′-[(4-formylphenoxy)methyl]biphenyl-2-carbonitrile or ethyl (4- formylphenoxy)acetate (0.0006 mol), 2, 4-thiazolidinedione or barbituric acid (1 equiv.), benzoic acid (30% mol), and piperidine (30% mol) in 2 mL of toluene was refluxed with continuous removal of water formed during the reaction using a Dean-Stark apparatus for 3–4 h. The reaction mixture was cooled, and the yellow solid was filtered off and dried to afford the corresponding compound.

4′-({4-[(Z)-(2,4-dioxo-1,3-thiazolidin-5-ylidene) methyl]phenoxy}methyl)-1,1′-biphenyl-2-carbonitrile (1)

Yield: 80%, mp: 235.6–236.8 °C. ^{1}H NMR (400 MHz, DMSO-*d*6) δ: 5.25 (2H, s, CH_2), 7.18 (2H, d, J_o = 9.2 Hz, H-2′, H-6′), 7.53–7.64 (5H, m, H-4, H-3′, H-5, H-3″, H-5″), 7.59 (1H, s, NH), 7.71 (1H, C=CH), 7.74–7.78 (4H, m, H-5,H-6, H-2″, H-6″), 7.95 (1H, dd, J_o = 8.0, J_m = 1.2 Hz, H-3, ppm; ^{13}C NMR (100 MHz, DMSO-*d*6) δ: 69.4 (CH_2), 110.6 (C-2), 116.1 (C-2′, C-6′), 119.1 (C=C), 121.4 (C-4′), 126.3 (C-6), 128.6(C-3″, C-5″), 128.7 (CN), 129.3(C-3′, C5′), 130.6 (C-5), 131.8 (C-4″) 132.5 (C-2″, C-6″), 134.0 (C-4), 134.3 (C-3), 137.5 (C-1″), 137.9 (C-1), 144.6 (HC=C), 160.4 (C-1″), 168.5 (O=C-S), 168.7 (O=C-N) ppm; MS/FAB$^+$: *m/z* 413 (M + H$^+$). Anal. Calcd for $C_{24}H_{16}N_2O_3S$: C, 69.89; H, 3.91; N, 6.79; S, 7.77. Found: C, 69.92; H, 3.92; N, 6.81; S, 7.79.

4′-({4-[(2,4,6-trioxotetrahydropyrimidin-5(2H)-ylidene)methyl]phenoxy}methyl)biphenyl-2-carbonitrile (2)

Yield: 73%, mp: 267 °C (dec). ^{1}H NMR (400 MHz, DMSO-*d*6) δ: 5.32 (2H, s, CH_2), 6.82 (2H, d, J_o = 9.2 Hz, H-2′, H-6′), 7.17 (dd, 1H, J_o = 8.8, J_m = 2 Hz, H-4)7.94 (dd, 1H, J_o = 7.6, J_m = 1.6 Hz, H-6), 7.76–7.80 (m, 2H, H-3, H-5), 7.57–7.64 (m, 4H, H-2, H-6″, H-3″, H-5″), 8.24 (1H, s, C=CH), 8.36 (2H, dd, J_o = 9.2 Hz, H-3′, H-5′), 10.0 (2H, 2NH) ppm; ^{13}C NMR (100 MHz, DMSO-*d*6) δ: 74.4 (CH_2), 115.3 (C-2), 115.4 (C-2′, C-6′), 119.9 (C=C), 120.9 (C-4′), 123.8 (C-6), 130.6 (C-3″, C-5″), 133.1 (C-5), 133.4 (C-3′, C-5′), 133.5 (CN), 133.9 (C-2″, C-6″), 135.3 (C-4), 138.8 (C-3), 139.7 (C-4″), 142.6 (C-1″). 149.3 (C=O),

155.4 (HC=C), 156.8 (C-1), 167.4 (N-C=O), 167.6 (N-C=O), 169.1 (O-C=O) ppm; MS/FAB$^+$: *m/z* 424 (M + H$^+$). Anal. Calcd for $C_{25}H_{17}N_3O_4$: C, 70.91; H, 4.05; N, 9.92. Found: C, 70.88; H, 4.08; N, 9.97.

Ethyl {4-[(Z)-(2,4-dioxo-1,3-thiazolidin-5-ylidene) methyl]phenoxy}acetate (3)

Yield: 75%, mp: 191.9–193.7 °C. ^{1}H NMR (400 MHz, DMSO-*d*6) δ: 1.19 (3H, t, CH_3), 4.15 (2H, q, CH_2), 4.85 (2H, s, CH_2), 7.07 (1H, NH), 7.07 (2H, dd, J_o = 8.8 Hz, J_m = 1 Hz, H-2′, H-6′), 7.53 (2H, dd, J_o = 8.8 Hz, J_m = 1 Hz, H-3′, H-5′), 7.72 (1H, s, CH) ppm; ^{13}C NMR (100 MHz, DMSO-*d*6) δ: 14.5 (CH_3), 61.2 (CH_2), 65.1 (CH_2), 115.9 (C-2, C-6), 121.2 (C=C), 126.6 (C-4), 132.1 (HC=C), 132.4 (C-3, C-5), 159.6 (C-1), 167.9 (N-C=O), 168.4 (O-C=O), 168.8 (S-C=O) ppm; MS/FAB$^+$: *m/z* 308 (M + H$^+$). Anal. Calcd for $C_{14}H_{13}NO_5S$: C, 54.71; H, 4.26; N, 4.56; S, 10.43. Found: C, 54.73; H, 4.25; N, 4.52; S, 10.39.

Ethyl {4-[(2,4,6-trioxotetrahydropyrimidin-5(2H)-ylidene)methyl]phenoxy}acetate (4)

Yield: 78%, mp: 210.1–212.5 °C. ^{1}H NMR (400 MHz, DMSO-*d*6) δ: 1.19 (3H, t, CH_3), 4.15 (2H, q, CH_2), 4.64 (2H, s, CH_2), 6.69 (2H, dd, J_o = 8.8 Hz, J_m = 1 Hz, H-2′, H-6′), 8.23 (1H, S, CH), 8.31 (2H, dd, J_o = 8.8 Hz, J_m = 1 Hz, H-3′, H-5′), 11.26 (2H, 2NH) ppm; ^{13}C NMR (100 MHz, DMSO-*d*6) δ: 14.4 (CH_3), 61.3 (CH_2), 65.2 (CH_2), 113.9 (C-2, C-6), 116.5 (C=C), 126.2 (C-4), 137.6 (C-3, C-5), 150.7 (C=O), 152.1 (HC=C), 161.9 (C-1), 162.6 (N-C=O), 164.3 (N-C=O), 169.3 (O-C=O) ppm; MS/FAB$^+$: *m/z* 319 (M + H$^+$). Anal. Calcd for $C_{15}H_{14}N_2O_6$: C, 56.60; H, 4.43; N, 8.80. Found: C, 56.78; H, 4.43; N, 8.87.

Synthesis of 4′-[(4-formylphenoxy)methyl]-1,1′-biphenyl-2-carbonitrile (5)

A mixture of 4-hydroxybenzaldehyde (0.100 g, 0.0008 mol) and potassium carbonate (0.169 g, 0.0012 mol, 1.5 equiv.) was dissolved in acetone (10 mL) and was stirred at room temperature. After 30 min, 4′-bromomethylbiphenyl-2-carbonitrile (0.22 g, 0.0008 mol, 1.01 equiv.) was added in small portions and stirred for 2 h. After the completion of the reaction, the solvent was removed under reduced pressure, and the resulting solid washed with water to extract the formed KBr. The crude solid product was then recrystallized from acetone.

Yield: 77%, mp: 137.1–139.6 °C. ^{1}H NMR (400 MHz, DMSO-*d*6) δ: 5.32 (2H, s, CH_2), 7.25 (2H, d, J_o = 8.4 Hz, H-2′, H-6′), 7.57 (d, 1H, J_m = 1.2 Hz, H-4), 7.58–7.68 (4H, m, H-2″, H-3″, H-5″, H-6″), 7.74–7.78 (2H, dt, J_o = 8.0, J_m = 1.2 Hz, H-5, H-6), 7.89 (2H, dd, J_o = 8.4, H-3′, H-5′), 7.96 (d, 1H, J_o = 8.0 Hz, H-3) 9.88 (1H, O=C-H) ppm; ^{13}C NMR (100 MHz, DMSO-*d*6) δ: 69.6 (CH_2), 110.6 (C-2), 115.7 (C-2′, C-6′), 128.6 (C-3″, C-5″), 128.7 (C-4′), 129.3(C-3′, C-5′), 129.5 (CN), 130.1 (C-4″), 130.2 (C-5), 130.6 (C-6), 132.3 (C-2″, C-6″), 133.9 (C-4), 134.3 (C-3), 137.3 (C-4′), 137.9 (C-1″), 144.5 (C-1), 163.6 (C-1′), 191.7 (H-C=O) ppm; MS/FAB$^+$: *m/z* 314 (M + H$^+$).

Synthesis of Ethyl (4-formylphenoxy)acetate (9)

A mixture of 4-hydroxybenzaldehyde (0.100 g, 0.0008 mol) and potassium carbonate (0.169 g, 0.0012 mol, 1.5 equiv.) was dissolved in acetone (10 mL) and was stirred at room temperature. After 30 min, ethyl bromoacetate (0.138 g, 0.0008 mol, 1.01 equiv.) was added dropwise and stirred for 4 h. After the completion of the reaction, the solvent was removed under reduced pressure, and the oily residue washed with water to extract the formed KBr. The oily product was then purified by column chromatography.

Yield: 65%, oil. ^{1}H NMR (400 MHz, DMSO-*d*6) δ: 1.62 (3H, t, CH_3), 3.33 (2H, q, CH_2), 5.10 (2H, s, CH_2), 6.85 (2H, dd, J_o = 9.2 Hz, H-2′, H-6′), 8.38 (2H, dd, J_o = 9.2 Hz, J_m = 1 Hz, H-3′, H-5′), 9.99 (1H, s, O=C-H) ppm; ^{13}C NMR (100 MHz, DMSO-*d*6) δ: 22.5 (CH_3), 69.1 (CH_2), 69.6 (CH_2), 115.1 (C-2, C-6), 130.5 (C-4), 134.2 (C-3, C-5), 162.8 (C-1), 164.3 (O-C=O), 206.9 (H-C=O) ppm; MS/FAB$^+$: *m/z* 209 (M + H$^+$).

Biological evaluation

In vitro PPAR assay

3T3-L1 fibroblasts (9 × 10^5 cells per well) were cultured in 6-well plates (Corning Incorporated, Corning, Corning, NY, USA) in Dulbecco's modified Eagle's medium supplemented with 25 mM glucose, 10% fetal bovine serum (v/v), 1 mM sodium pyruvate, 2 mM glutamine, 0.1 mM non-essential amino acids, and gentamicin, in a 5% CO_2 humidified atmosphere, at 37 °C. After 2 days of confluence, the cells were differentiated to the adipocyte phenotype with 0.5 mM 3-isobutyl-1-methylxanthine, 0.25 μM dexamethasone acetate, and 0.8 μM insulin, for 48 h, followed by insulin alone for 48 h more. The culture medium without insulin was changed every 2 days during 8 days of differentiation (12). To determine the effect of compounds on PPARs and GLUT-4 expression, the cells were treated by 24 h.

RNA was isolated from cultured cells using a TriPure isolation reagent (Invitrogen, Paisley, UK). Absorbance was measured at 260 and 280 nm for each RNA sample, and the absorbance ratio (260–280 nm) was 1.9 ± 0.2. To confirm RNA integrity, 1 μg was run in 1% agarose gel. RNA was stained with ethidium bromide and visualized using an Image Gel-Logic 212 Pro (Kodak/Caaresream, Rochester, New York, USA). Two major ribosomal bands (28S and 18S rRNA) but no degraded RNA were detected (data not shown). Two micrograms of total RNA were reverse-transcripted using the ImProm II reverse transcrip-

tion system (Promega, Madison, WI, USA), the reaction (20 μL) was incubated in a thermocycler Select Cycler (BioProducts, West Palm Beach, FL, USA), following the cycle program: incubation at 25 °C for 5 min, extension at 42 °C for 55 min. The enzyme was inactivated at 70 °C, for 15 min, and finally, samples were cooled to 4 °C, for 5 min. Then 1/10 volume of each RT reaction was amplified with SYBR Green master mix (Roche Molecular Biochemicals, Mannheim, Germany) containing 0.5 mM of customized primers for PPAR-γ (F-CCAGAGTCTGCTGATCTGCG; R-GCCACCTCTTTGCTCTGCTC; Gene Bank NM_011146.1), PPAR-α (F- ATGCCAGTACTGCCGTTTTC; R-GGCCTTGACCTTGTTCATGT; Gene Bank NM_011144), GLUT-4 (F- GATTCTGCTGCCCTTCTGTC; R- ATTGGACGCTCTCTCTCCAA; Gene Bank NM_009204.2), as well as Fast Start enzyme, PCR buffer and 3.5 mM $MgCl_2$, in a final volume of 10 μL, the reactions were measured in a Rotor-Gene real-time (Corbett Life Science, Concorde, NSW, Australia). PCR was conducted using the following cycling conditions: pre-incubation and denaturation at 95 °C during 10 min. The threshold cycles (*Ct*) were measured in separate tubes and in duplicate (13). The identity and purity of the amplified products was checked by electrophoresis on 2% agarose gel. The melting curve was analyzed at the end of amplification following SYBER Green kit conditions, as indicated by the company (Roche Molecular Biochemicals). To ensure the quality of the measurements, each assay included a negative control for each gene. The amount of mRNA for each adipokine was normalized according to the amount of mRNA encoding ribosomal protein 36B4 (F-AAGCGCGTCCTGGCATTGTCT; R-CCGCAGGGGCAGCAGTGGT; Gene Bank NM_007475.2).

The ΔCt values were calculated in every sample for each gene of interest as follows: Ctgene of interest−Ctreference gene with β-actin as the reference gene (mRNA of reference remained stable throughout the experiments). Relative changes in the expression level of one specific gene ($\Delta\Delta Ct$) were calculated as ΔCt of the test group minus ΔCt of the control group and then presented as $2-\Delta\Delta Ct$.

In silico docking studies

DISCOVERY STUDIO, version 3.5, (Accelrys Inc., San Diego, CA, USA), and PYMOL 1.0 were used for visualization. The crystal structure of PPARα and PPARγ was retrieved from the PDB with the accession codes 1I7G and 1I7I, respectively. Docking calculations were conducted with AUTODOCK, version 4.2 (14). In short, AUTODOCK performs an automated docking of the ligand with user-specified dihedral flexibility within a protein rigid binding site. The program performs several runs in each docking experiment. Each run provides one predicted binding mode. All water molecules and also tesaglitazar (crystallographic ligand) were removed from the crystallographic structure, and all hydrogen atoms were added. For all ligands and proteins, Gasteiger charges were assigned and non-polar hydrogen atoms were merged. All torsions were allowed to rotate during docking. The auxiliary program AUTOGRID generated the grid maps. Each grid was centered at the crystallographic coordinates of the crystallographic compound. The grid dimensions were 60 × 60 × 60 Å with points separated by 0.375 Å. The Lamarckian genetic algorithm was applied for the search using default parameters. The number of docking runs was 25. After docking, all solutions were clustered into groups with RMSD lower than 2.0 Å. The clusters were ranked by the lowest energy representative of each cluster.

Validation was performed in AUTODOCK 4.2 using PDB proteins 1I7G (PPARα) and 1I7I (PPARγ). The X-ray crystal structure (Tesaglitazar) was built and docked within the active site region formed by PPARα residues: Cys276, Ser280, Tyr314, Leu321, Val332, His440; and PPARγ residues: Tyr464 and Cys285, Ser289, His323, Ile341, Met364, His449, and Tyr473. This validation was carried out based on the important interactions made by the ligand bound within the active site residues indicating that the parameters for docking simulations are good in reproducing theses interactions between the X-ray crystal structure with both receptors.

In vivo studies

Male Wistar rats weighing 200–250 g bodyweight were housed at standard laboratory conditions and fed with a rodent pellet diet and water *ad libitum*. They were maintained at room temperature and at a photoperiod of 12 h day/night cycle. Animals described as fasted were deprived of food for 16 h but had free access to tap water. All animal procedures were conducted in accordance with our Federal Regulations for Animal Experimentation and Care (SAGARPA, NOM-062-ZOO-1999, México) and approved by the Institutional Animal Care and Use Committee based on US National Institute of Health publication (No. 85-23, revised 1985).

Induction of diabetes

Streptozotocin (STZ) was dissolved in citrate buffer (pH 4.5) and nicotinamide was dissolved in normal physiological saline solution. Non-insulin-dependent diabetes mellitus rat model was induced in overnight fasted rats by a single intraperitoneal injection of 65 mg/kg STZ, 15 min after the i.p. administration of 110 mg/kg of nicotinamide (15). Hyperglycemia was confirmed by the elevated glucose concentration in plasma, determined at 72 h by glucometer. The animals with blood glucose concentration higher than 250 mg/dL were used for the antidiabetic screening.

Antidiabetic assay (non-insulin-dependent diabetes mellitus rat model)

The diabetic animals were divided into groups of five animals each (n = 5). Rats of experimental groups were

administered a suspension of the compound **1** (prepared in 1% Tween 80) orally (50 mg/kg body weight). A control group animal was also treated with 1% Tween 80. Glibenclamide (5 mg/kg) was used as hypoglycemic reference drug. Blood samples were collected from the caudal vein at 0, 1, 3, 5, and 7 h after vehicle, sample and drug administration. Blood glucose concentration was estimated by the enzymatic glucose oxidase method using a commercial glucometer (Accu-Chek, Performa; Roche®). The percentage variation of glycemia for each group was calculated in relation to the initial (0 h) level, according to the formula, %Variation of glycemia = $[(G_x - G_0)/G_0] \times 100$, where G_0 were initial glycemia values, and G_x were the glycemia values at +1, +3, +5, and +7 h, respectively (14). All values were expressed as mean ± SEM. Statistical significance was estimated by analysis of variance (ANOVA), $p < 0.05$ and $p < 0.01$ implies significance.

Results and Discussion

Chemistry

Title compounds **1**–**4** were prepared in a two-step reaction. Starting from 4-hydroxybenzaldehyde (**7**), it was alkylated with 4-bromomethylbiphenyl-2-carbonitrile (**6**) under S_N2 conditions to give rise to the aldehyde **5** (Scheme 1).

The aldehyde **5** was condensed with 2,4-thiazolidinedione or barbituric acid, following Knoevenagel reaction conditions to afford compounds **1** and **2**, respectively (Scheme 2).

For the rest of compounds, the treatment of aldehyde **7** with ethyl bromoacetate (**8**) provided ester **9,** which was reacted with 2,4-thiazolidinedione or barbituric acid, using Knoevenagel reaction once again, to obtain compounds **3** and **4**, respectively (Scheme 3).

All compounds were recovered with 73–80% yields. Compounds were purified by recrystalization or by column chromatography. The chemical structures of the synthesized compounds were confirmed on the basis of their spectroscopic and spectrometric data (NMR and mass spectra), and their purity ascertained by microanalysis.

The in vitro *part*

Relative expression of PPARα and PPARγ

Results presented in Figure 2A–C shows that compound **1** increase significantly the levels of relative expression for PPARγ (about fivefold), PPARα (sixfold), and GLUT4 (threefold) mRNA's. The activation of PPARγ could decrease the glucose serum levels in diabetic patients due to the reduction in insulin resistance. Meanwhile, the activation of PPARα is known to be effective in reducing serum triglyceride levels (16). Our data also suggest that compound **1** can induce GLUT4 expression.

Skeletal muscle glucose uptake is the rate-limiting step of glucose utilization, and insulin-dependent and insulin-independent signaling pathways physiologically regulate it, both leading to the translocation of GLUT4 glucose transporter to the plasma membrane. Several evidences indicate that the levels of GLUT4 expression in skeletal muscle are crucial for the regulation of total body glucose homeostasis (17,18).

The designed scaffold hop from 2,4-thiazolidinedione and barbituric acid did not retain the full biological effect,

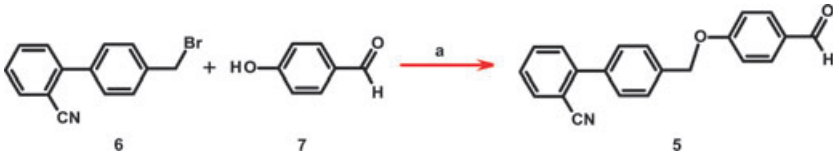

Scheme 1: Synthesis of precursor **5**. a) K_2CO_3, acetone, reflux.

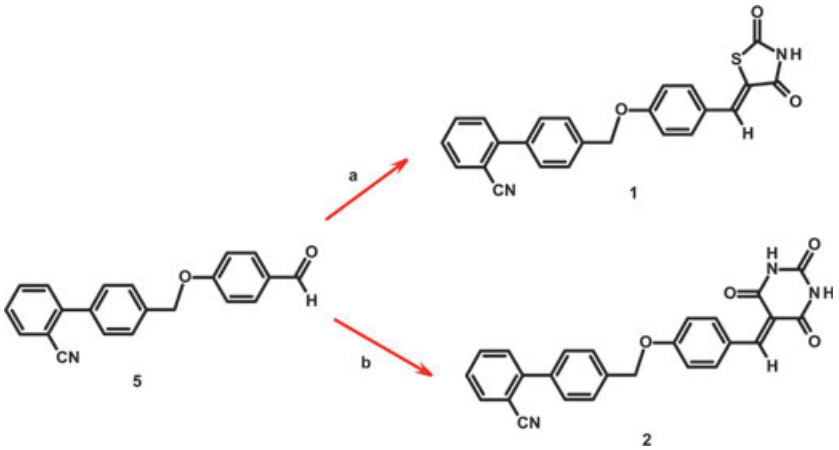

Scheme 2: Synthesis of compounds **1** and **2.** a) 2,4-thiazolidinedione, benzoic acid (cat), piperidine (cat), toluene, reflux; b) barbituric acid, benzoic acid (cat), piperidine (cat), toluene, reflux.

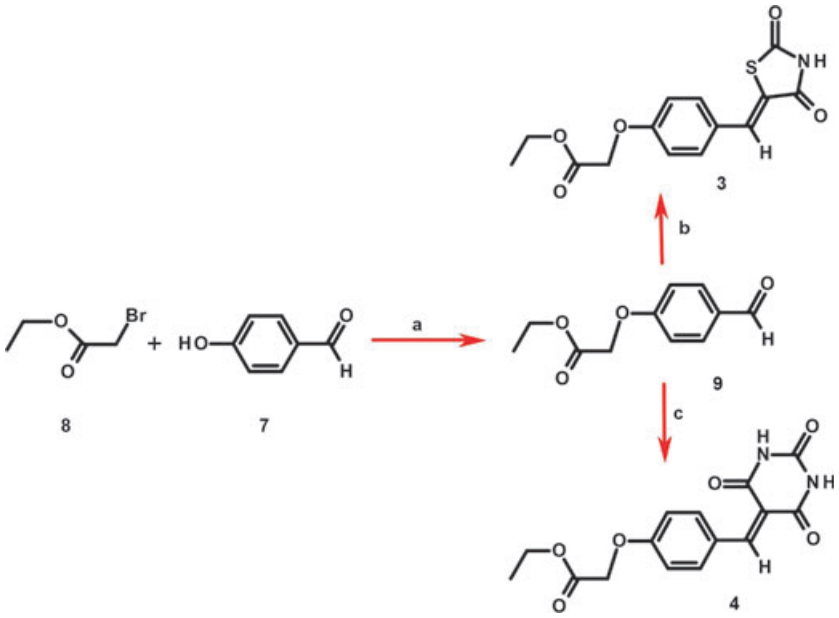

Scheme 3: Synthesis of compounds **3** and **4**. a) K_2CO_3, acetone, reflux; b) 2,4-thiazolidinedione, benzoic acid (cat), piperidine (cat), toluene, reflux; c) barbituric acid, benzoic acid (cat), piperidine (cat), toluene, reflux.

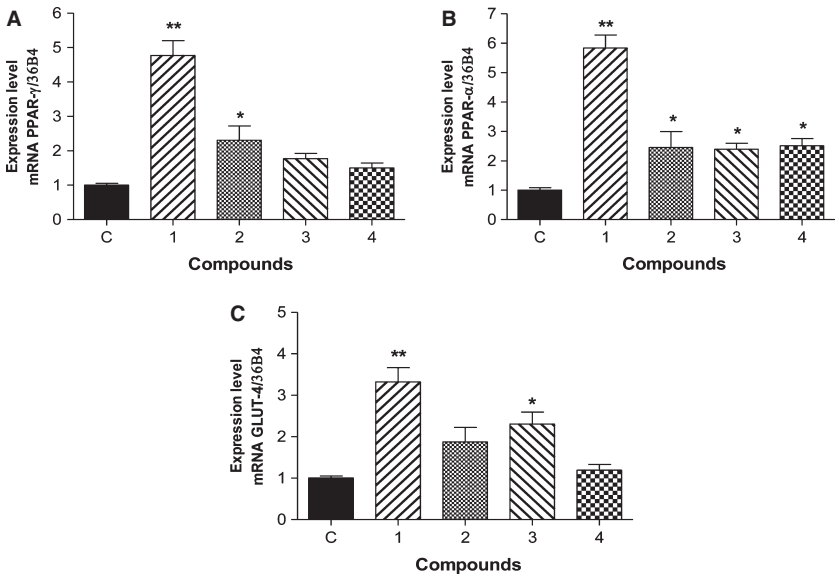

Figure 2: Effect of compounds on expression of: mRNA PPARγ (A), PPARα (B), and GLUT4 (C). Results are mean ± SEM (n = 6) *p < 0.05 compared with control (C). **p < 0.01 compared with control group. PPAR, peroxisome proliferator-activated receptor.

converting structures **1** and **2** into activity cliffs (chemical compounds with highly similar structures but significantly different biological activities) (19). It is possible that lack of activity for compounds **3** and **4** in to the PPARγ could be related to low lipophilic tail showed by these structures.

The in silico *part*

Molecular docking of compound 1 with PPARα and PPARγ

The aim of the molecular docking tools is to map the possible drug–receptor interactions to explain the activity shown to assist to rational drug design. Compound **1** was docked into the catalytic site of the human PPARα and PPARγ using the program AUTODOCK 4.2. The docking protocol was validated by re-docking of co-crystal ligand Tesaglitazar in both PPAR's isoforms. After re-docking, the root mean square (RMS) deviation between the co-crystal ligand and the docked structure was 0.99 Å to PPARα and 1.19 Å to PPARγ.

The compound **1** exhibited three hydrogen bonds between oxygen and sulfur atoms from 2,4.thiazolidinedione and several amino acids found in the active site of PPARα, such as Ser280, Tyr314, His440, showing a binding free energy of −11.04 Kcal/mol (Figure 3).

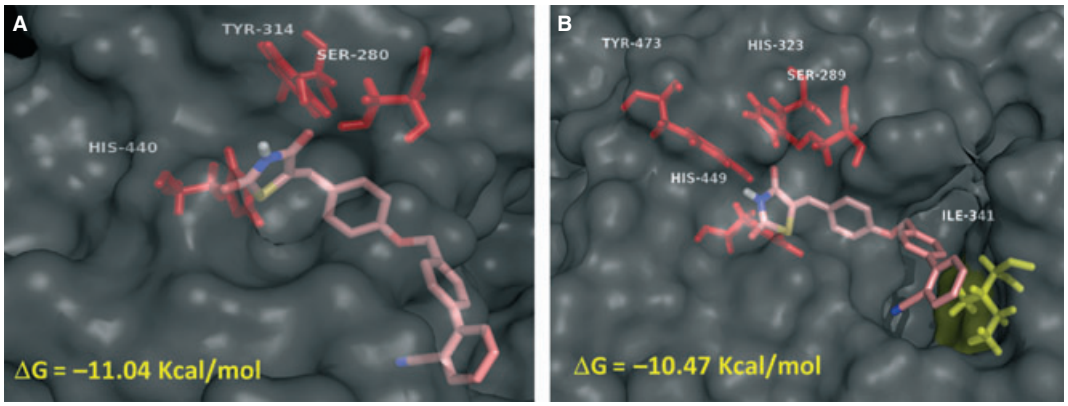

Figure 3: Binding model of **1** in the active site of (A) PPARα and (B) PPARγ. Stick representation of side chains (in red), shows the residues that participate in the hydrogen bond network. Residue making van der Waals contacts is in yellow. PPAR, peroxisome proliferator-activated receptor.

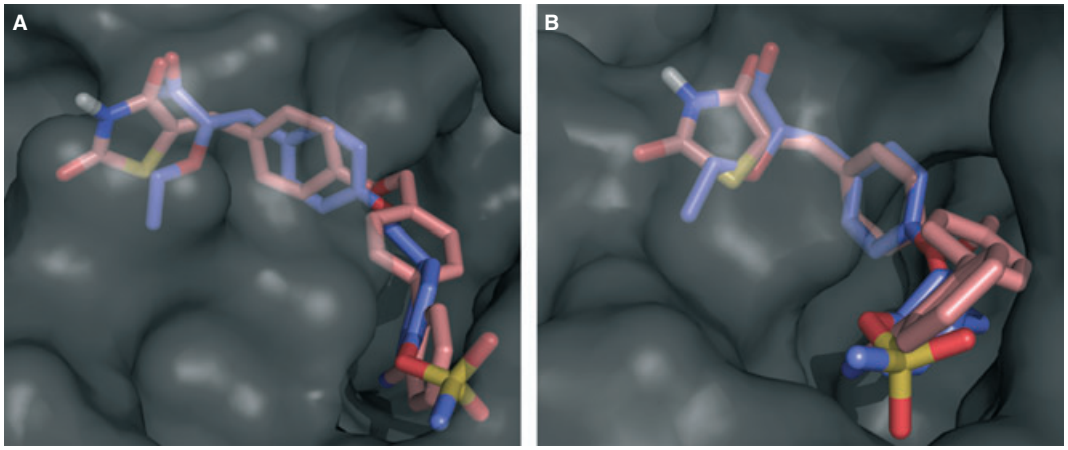

Figure 4: Comparison of docked **1** and co-crystal ligand (Tesaglitazar) into the active binding site of PPARα (A) and PPARγ (B). They represent the lowest energy conformation estimated by AUTODOCK4.2. PPAR, peroxisome proliferator-activated receptor.

Compound **1** also showed four hydrogen interactions between the 2,4-thiazolidinedione core and the PPARγ residues Ser289, His323, His449, and Tyr473, showing binding free energy of −10.47 Kcal/mol. An extra π-σ interaction was found between 2-cyanophenyl group and Ile341 (Figure 3). The molecular docking study revealed that compound **1** docked into PPAR α and γ exhibited hydrogen bonds via O=C and -S- atoms with important residues involved in the interaction shown by a significant dual receptor agonist (Tesaglitazar). This could explain its relevant activity on both receptors.

Figure 4 shows a comparison of the binding mode of the most active compound with tesaglitazar. In addition, compound **1** share the same binding pattern and pharmacophoric interactions as the co-crystal ligand of PPAR's. It is notable the three-dimensional similarity of the binding models of the compound **1** and Tesaglitazar.

Figure 5 depicts the 2D interactions maps of compound **1** and tesaglitazar. Hydrogen bond network is conserved by **1**, with Ser, Tyr, and His in both PPAR isoforms. According to the models predicted by AUTODOCK4.2, the studied derivative binds into the active site of PPARα and PPARγ.

With these results, we propose that the features could be taking into consideration for designing novel dual PPAR α/γ modulators should consist of four parts:

(a)An acidic head group, such as thiazolidine-2,-4-dione, carboxylic acid, or related bioisoteres.

(b)A central aromatic backbone

(c)An extra-lipophilic aromatic region

(d)A flexible spacer that connects regions (b) and (c), and allow the structure to adopt specific conformation (Figure 6).

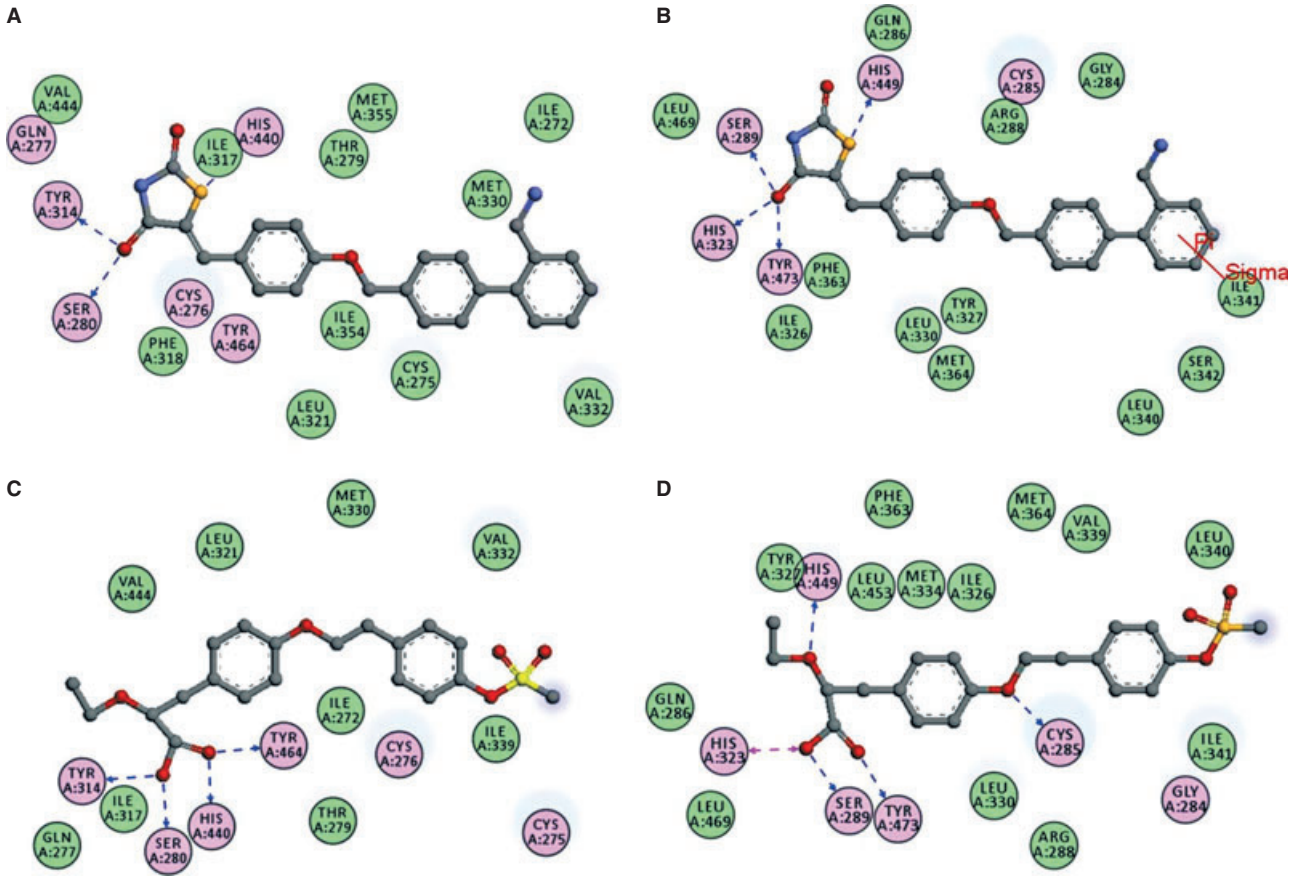

Figure 5: Two-dimensional interaction diagram of the predicted binding mode of compound **1** with: (A) PPARα and (B) PPARγ. It shows as reference, the corresponding 2-D interaction maps for tesaglitazar with (C) PPARα and (D) PPARγ. PPAR, peroxisome proliferator-activated receptor.

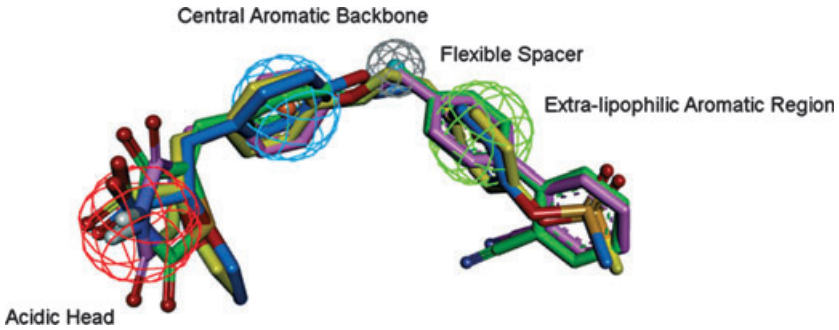

Figure 6: Overlay of bioactive conformations of Tesaglitazar (yellow: PPARα; blue: PPARγ) and compound **1** (purple: PPARα; green: PPARγ). It is remarkable that both compounds share the same binding pattern and pharmacophoric interactions with PPAR's. PPAR, peroxisome proliferator-activated receptor.

In silico *toxicology profile*

In silico prediction of toxicity has been performed in drug design and development to avoid the experimental study of potentially harmful substances. The toxicity parameters of the compound **1** and tesaglitazar were calculated through the ACD/TOXSUITE software, v. 2.95 (Table 1).

Cytochrome P450 isoform CYP3A4 is the major enzyme responsible for xenobiotic metabolism in human organism. Inhibition of CYP3A4 at clinically relevant concentration (IC_{50} < 10 μM) can lead to drug–drug interactions and undesirable adverse effects (20). Compound **1** showed satisfactory toxicity profiles, and its predictions of inhibition

Table 1: Toxicity profiles predicted for compound **1** and PPAR α/γ dual agonist tesaglitazar

	LD_{50} (mg/kg)				Probability of inhibition (IC_{50} or *Ki* <10 μM)				
	Mouse		Rat		CYP450 isoform				
Compound	i.p.	p.o.	i.p.	p.o.	3A4	2D6	2C9	1A2	hERG
1	520	1200	450	3200	0.25	0.03	0.26	0.02	0.58
Tesaglitazar	440	930	230	3600	0.22	0.05	0.15	0.02	0.01

hERG, human ether-a-go-go related gene; PPAR, peroxisome proliferator-activated receptor.

for the four isoforms of CYP450 were comparable than the reference compound tesaglitazar.

Cardiotoxicity of drug-like compounds associated with human ether-a-go-go (hERG) channel inhibition is becoming more and more common cause of drug candidates' attrition (21). Compound **1** showed low prediction of hERG channel inhibition at clinically relevant concentrations (*Ki* < 10 μM).

The acute toxicity of the chemical is defined as a dose that is lethal to 50% of the treated animals (LD_{50}). The acute toxicity can be viewed as a 'cumulative potential' to cause various acute effects and death of animals. In these predictions, compound **1** demonstrated similar calculated LD_{50} than tesaglitazar, showing low toxicity profiles.

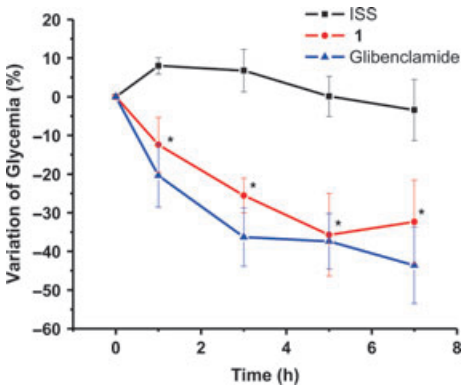

Figure 7: Effect of a single dose of **1** (50 mg/kg; intragastric, *n* = 5) in streptozotocin-nicotinamide-induced diabetes rat model. ISS, isotonic saline solution. *p < 0.05 versus ISS group.

The in vivo *part*

Antidiabetic activity of compound 1

Compound **1** was evaluated for *in vivo* antidiabetic activity using a STZ-nicotinamide non-insulin-dependent diabetes mellitus rat model (NIDDM) rat model (16,22). Glibenclamide was taken as hypoglycemic control. The hypoglycemic activity of **1** was determined using a 50 mg/kg single dose. Compound **1** demonstrated significant hypoglycemic activity ($p < 0.05$) compared with control, by lowering glycemia ranging from 12% to 35% (Table 2). The effect was sustained during the 7 h of experiment, and it was comparable with the hypoglycemic action showed by glibenclamide (Figure 7).

In our *in vivo* experiments, the increase in GLUT4 expression in rat could be associated with a marked decrease in glucose concentrations, confirming that the level of expression of this transporter in skeletal muscle may be crucial for the regulation of total body glucose homeostasis and insulin resistance.

Conclusions and Future Directions

We report the discovery of a thiazolidine-2,4-dione/biphenylcarbonitrile hybrid (**1**) as a promising antidiabetic compound, which shown significant increasing in the mRNA expression of PPAR α, PPAR γ, and also GLUT 4. This compound showed a good *in vivo* hypoglycemic effect. According to the docking models, compound **1** may bind into the active site of both PPAR's in the same manner as tesaglitazar does. The high *in vivo* hypoglycemic activity and the satisfactory toxicity profile predicted for this compound makes it a suitable lead to develop single entities with PPAR α/γ dual agonist that may confer potential use in the treatment of experimental diabetes.

Table 2: Percentage of variation of blood glucose concentration on streptozotocin-nicotinamide induced diabetic rats treated with compound **1**

		Percentage of variation of glycemia ± SEM (mg/dL)[a]				
Compound	Dose (mg/kg)	Zero hour	First hour	Third hour	Fifth hour	Seventh hour
1	50	0 ± 0.0	−12.42 ± 7.1	−25.55 ± 4.5	−35.72 ± 10.7	−32.36 ± 14.8
Glibenclamide	5	0 ± 0.0	−20.4 ± 8.17	−36.3 ± 7.55	−37.4 ± 7.16	−43.6 ± 9.9

[a]Values represent the mean ± SEM (*n* = 6). $p < 0.05$ compared with control group. The negative value indicates decrease in glycemia.

Acknowledgment

This work was supported in part by the Consejo Nacional de Ciencia y Tecnología (CONACyT) under grant No. 100608 and Facultad de Farmacia internal grant.

References

1. Lee C.H., Olson P., Evans R.M. (2003) Minireview: lipid metabolism, metabolic diseases, and peroxisome proliferator-activated receptors. Endocrinology;144:2201–2207.
2. Willson T.M., Brown P.J., Sternbach D.D., Henke B.R. (2000) The PPARs: from orphan receptors to drug discovery. J Med Chem;43:527–550.
3. Sharma A.K., Sk U.H., He P., Peters J.M., Amin S. (2010) Synthesis of isosteric selenium analog of the PPARbeta/delta agonist GW501516 and comparison of biological activity. Bioorg Med Chem Lett;20:4050–4052.
4. Wild S., Roglic G., Green A., Sicree R., King H. (2004) Global prevalence of diabetes: estimates for the year 2000 and projections for 2030. Diabetes Care;27:1047–1053.
5. Navarrete-Vazquez G., Ramírez-Martínez M., Estrada-Soto S., Nava-Zuazo C., Paoli P., Camici G., Escalante-García J., Medina-Franco J.L., López-Vallejo F., Ortiz-Andrade R. (2012) Synthesis, in vitro and in silico screening of ethyl 2-(6-substituted benzo[d]thiazol-2-ylamino)-2-oxoacetates as protein-tyrosine phosphatase 1B inhibitors. Eur J Med Chem;53:346–355.
6. Balakumar P., Rose M., Ganti S.S., Krishan P., Singh M. (2007) PPAR dual agonists: are they opening Pandora's Box? Pharmacol Res;56:91–98.
7. Adeghate E., Adem A., Hasan M.Y., Tekes K., Kalasz H. (2011) Medicinal chemistry and actions of dual and pan PPAR modulators. Open Med Chem J;5(Suppl. 2):93–98.
8. Cox S.L. (2006) Tesaglitazar: a promising approach in type 2 diabetes. Drugs Today (Barc);42:139–146.
9. Sundriyal S., Viswanad B., Ramarao P., Chakraborti A.K., Bharatam P.V. (2008) New PPARgamma ligands based on barbituric acid: virtual screening, synthesis and receptor binding studies. Bioorg Med Chem Lett;18:4959–4962.
10. Momose Y., Maekawa T., Yamano T., Kawada M., Odaka H., Ikeda H., Sohda T. (2002) Novel 5-substituted 2,4-thiazolidinedione and 2,4-oxazolidinedione derivatives as insulin sensitizers with antidiabetic activities. J Med Chem;45:1518–1534.
11. Momose Y., Maekawa T., Odaka H., Ikeda H., Sohda T. (2002) Novel 5-substituted-1H-tetrazole derivatives as potent glucose and lipid lowering agents. Chem Pharm Bull;50:100–111.
12. Garcia-Macedo R., Sanchez-Muñoz F., Almanza-Perez J.C., Duran-Reyes G., Alarcon-Aguilar F., Cruz M. (2008) Glycine increases mRNA adiponectin and diminishes pro-inflammatory adipokines expression in 3T3-L1 cells. Eur J Pharmacol;587:317–321.
13. Almanza-Perez J.C., Alarcon-Aguilar F.J., Blancas-Flores G., Campos-Sepulveda A.E., Roman-Ramos R., Garcia-Macedo R., Cruz M. (2010) Glycine regulates inflammatory markers modifying the energetic balance through PPAR and UCP-2. Biomed Pharmacother;64:534–540.
14. Morris G.M., Huey R., Lindstrom W., Sanner M.F., Belew R.K., Goodsell D.S., Olson A.J. (2009) Autodock4 and AutoDockTools4: automated docking with selective receptor flexibility. J Comput Chem;16:2785–2791.
15. Torres-Piedra M., Ortiz-Andrade R., Villalobos-Molina R., Singh N., Medina-Franco J.L., Webster S.P., Binnie M., Navarrete-Vázquez G., Estrada-Soto S. (2010) A comparative study of flavonoid analogues on streptozotocin-nicotinamide induced diabetic rats: quercetin as a potential antidiabetic agent acting via 11β-hydroxysteroid dehydrogenase type 1 inhibition. Eur J Med Chem;45:2606–2612.
16. Nevin D.K., Lloyd D.G., Fayne D. (2011) Rational targeting of peroxisome proliferating activated receptor subtypes. Curr Med Chem;18:5598–5623.
17. Tsao T.S., Li J., Chang K.S., Stenbit A.E., Galuska D., Anderson J.E., Zierath J.R., McCarter R.J., Charron M.J. (2001) Metabolic adaptations in skeletal muscle overexpressing GLUT4: effects on muscle and physical activity. FASEB J;15:958–969.
18. Zisman A., Peroni O.D., Abel E.D., Michael M.D., Mauvais-Jarvis F., Lowell B.B., Wojtaszewski J.F., Hirshman M.F., Virkamaki A., Goodyear L.J., Kahn C.R., Kahn B.B. (2000) Targeted disruption of the glucose transporter 4 selectively in muscle causes insulin resistance and glucose intolerance. Nat Med;6:924–928.
19. Méndez-Lucio O., Pérez-Villanueva J., Castillo R., Medina-Franco J.L. (2012) Activity landscape modeling of PPAR ligands with dual-activity difference maps. Bioorg Med Chem;20:3523–3532.
20. Xu L., Chen Y., Pan Y., Skiles G.L., Shou M. (2009) Prediction of human drug-drug interactions from time-dependent inactivation of CYP3A4 in primary hepatocytes using a population-based simulator. Drug Metab Dispos;37:2330–2339.
21. Taboureau O., Jørgensen F.S. (2011) In silico predictions of hERG channel blockers in drug discovery: from ligand-based and target-based approaches to systems chemical biology. Comb Chem High Throughput Screen;14:375–387.
22. Moreno-Díaz H., Villalobos-Molina R., Ortiz-Andrade R., Díaz-Coutiño D., Medina-Franco J.L., Webster S.P., Binnie M., Estrada-Soto S., Ibarra-Barajas M., León-Rivera I., Navarrete-Vázquez G. (2008) Antidiabetic activity of *N*-(6-substituted-1,3-benzothiazol-2-yl)benzenesulfonamides. Bioorg Med Chem Lett;18:2871–2877.